# P2.153 A numerical study of the evolution of the surface layer during the rapid intensification of Hurricane Bill (2009)

J. Zhang[1,2], A. Aksoy[1,2], S. Lorsolo[1,2], R. Rogers[1], E. Uhlhorn[1],
J. Cione[1], J. Dunion[1], J. Kaplan[1], K. Yeh[1,2], X. Zhang[1,2], S. Gopalakrishnan[1],
T. Quirino[1], J. Cangialosi[3], and F. Marks[1]
[1]Rosenstiel School of Marine and Atmospheric Science, University of Miami, FL, USA
[2]NOAA/AOML, Hurricane Research Division, Miami, FL, USA
[3]NOAA/ /NWS/NCEP/TPC, National Hurricane Center, Miami, FL, USA

**Background and Motivation:**

The rapid intensification (RI) of tropical cyclones is a complicated problem which has not been well-understood. It is very challenging to predict RI operationally, because it involves multiscale physical processes that include environmental, vortex, convective, turbulent and microphysical scales. The large-scale environmental influence has been found to play an important role in predicting RI (Kaplan et al. 2009). Using data from the operational Statistical Hurricane Intensity Prediction Schemes (SHIPS), Kaplan et al. (2009) developed a rapid intensity index to estimate the probability of RI over a 24 hour time interval, suggesting that nearly 35% of the skill of RI prediction for the Atlantic basin can be captured by the large-scale environmental processes.

It is assumed that the remaining skill (65%) of RI prediction, not limited by predictability constraints, is related to vortex- and convective-scale structure and dynamics, boundary layer turbulence, and air-sea interaction. Much research has focused on the vortex- and convective-scale structures important in intensification (e.g., Rogers 2010, Reasor et al. 2009, Nolan et al. 2007, Kelley et al 2004, Kossin and Eastin 2001). What has not been studied as extensively is the structure and evolution of the boundary layer and air-sea exchange processes prior to and during RI. The purpose of this study is to study boundary-Layer and air-sea exchange processes prior to, during, and after an RI event to determine if these processes may play a role in initiating RI.

**Simulation description:**

We used data from a real-time 3-km simulation of Hurricane Bill (2009) using the experimental version of Hurricane Weather and Forecasting (HWRF-X) model that is being developed at the Hurricane Research Division (Yeh et al. 2010). This is an uncoupled model that contains parameterizations for microphysical, boundary layer, and radiative processes on the 3-km mesh. It uses the standard HWRF initial conditions and GFS forecast lateral boundary conditions. Note that the exchange coefficients for momentum and enthalpy transfer in the surface layer scheme are the same as those used in the Operational GFDL model, which are different from those based on recent flux observations (Black et al. 2007, Zhang et al. 2008). Sea-surface temperature is based on GFS initial condition and is fixed in time.

**Model verification:**

The simulated track and intensity of Hurricane Bill are shown in Figs. 1 and 2, respectively. The model is able to simulate the track of Bill very well. The simulated intensity (Fig. 2) is also close to (~<10 kts) the observed (best track), including the timing and magnitude of RI beginning at hour 48 in the simulation. Three stages of the lifecycle of Bill are identified here: pre-rapid intensification (PR, 30-48 hour forecast), rapid intensification (RI, 48-72 hour forecast) and steady-state (SS, 72-96 hour forecast). Fig. 3 shows the surface wind from the simulation compared to the H*Wind analysis at the 92 forecast time. The magnitude and azimuthal location of the peak wind compares well, though the radius of maximum wind in the simulated storm is larger than that produced in H*Wind.

In particular, the simulated vortex is broader and shallower. An east-west cross section from the radar and simulation (Fig. 5) shows that while the inner core of the simulated vortex was generally well-represented, the pronounced asymmetry outside the eyewall seen in the radar analysis is not seen in the model. In general, though, the model does a good job at reproducing the evolution of Bill, even if some aspects of the structure were incorrect.

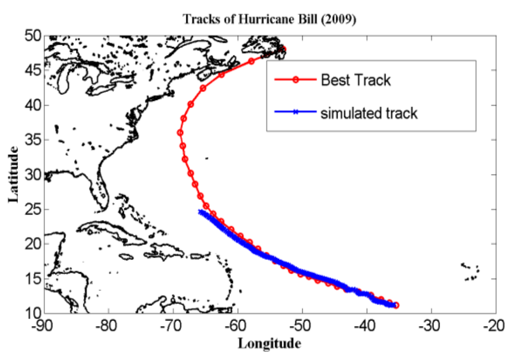


*Fig. 1: Forecast hurricane track.*

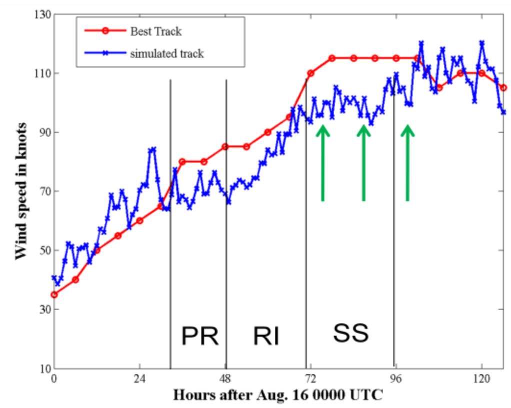


*Fig. 2: Forecast intensity. Times when aircraft was sampling storm shown by green arrows.*

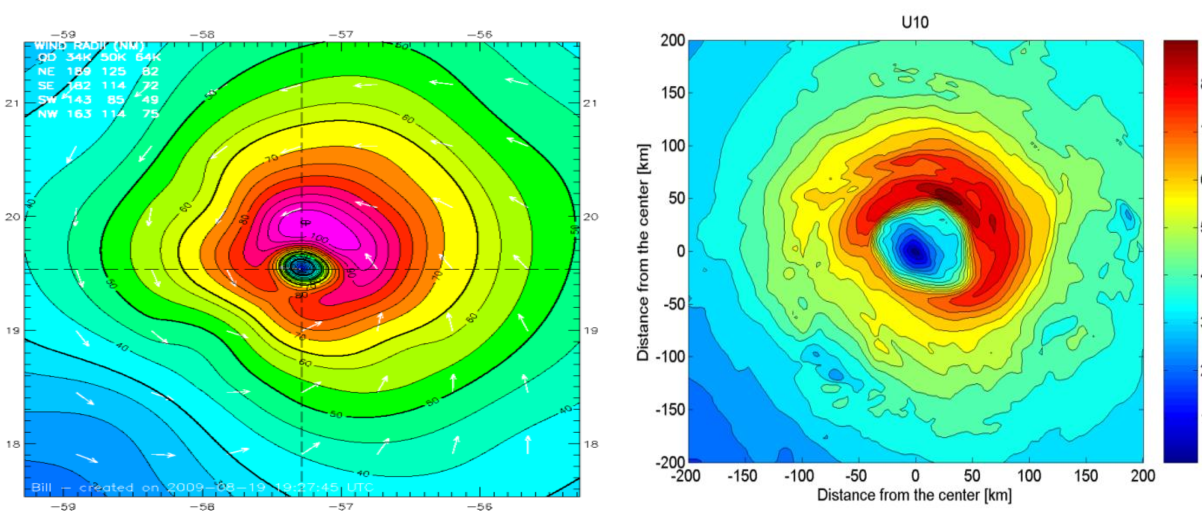


*Fig. 3: Comparison of the surface wind simulated at 92 hours to the HWind analysis at the same time (shaded, kt).*

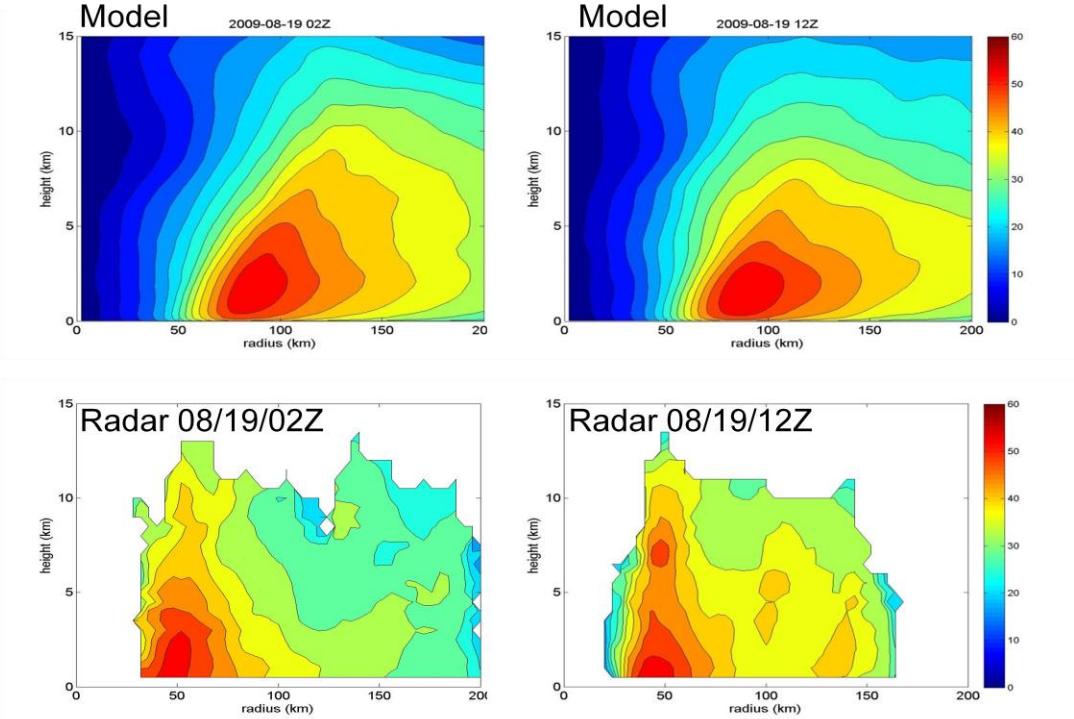


*Fig. 4: Comparisons showing the tangential component wind velocity from the model and the coincident radar data.*

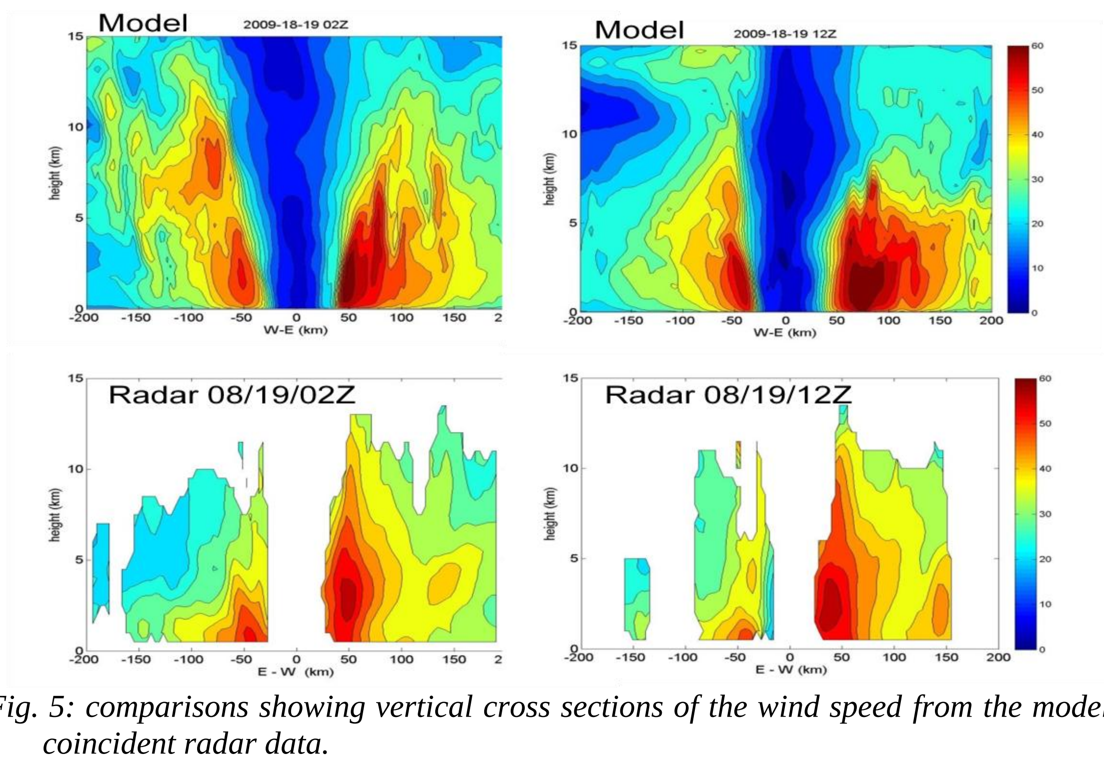


*Fig. 5: comparisons showing vertical cross sections of the wind speed from the model and coincident radar data.*

During HRD's 2009 field program, NOAA aircraft observations were collected during the SS stage (Fig. 2). The radar data collected at three different times are used to compare the simulated axisymmetric primary circulation with the observed (Fig. 4). The general structure of the simulated vortex is similar to that shown in the radar observations, but there are a few notable exceptions.

**Comparison of vortex scale structure during PR, RI and SS:**

We focus on 3 stages, PR (30-48 hour forecast), RI (48-72hour forecast) and SS (72-96 hour forecast) from the HWRF-X simulation. The time-averaged r-z mean fields are computed for the three periods (PR, RI and SS).

Comparisons of the kinematic structure are shown in Fig. 6. It can be seen that the primary circulation strengthens from PR to RI to SS. However, the secondary circulation for RI and SS are comparable. The vertical velocity during RI is much stronger than the PR and SS periods.

Comparisons of the time-averaged r-z mean thermodynamic fields during the three stages are shown in Fig. 7. It appears that there is no considerable difference in the temperature and specific humidity fields between PR, RI and SS. The mixed layer is slightly shallower during RI compared to PR and SS. The relative humidity in the eyewall region is higher during RI compared to PR and SS.

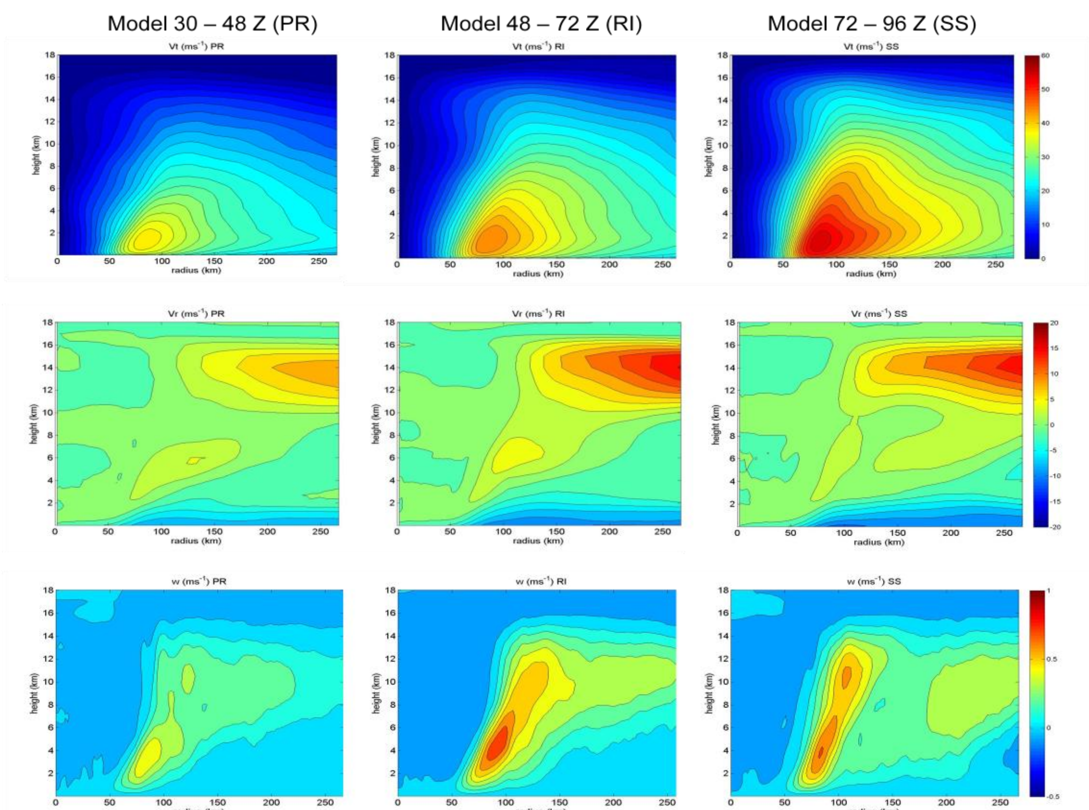


*Fig. 6: Comparison of the time-averaged simulated fields during the three stages of Bill's life cycle: PR, RI, and SS. The upper three panels show the tangential wind velocity, the middle panels show the radial wind velocity, and the lower panels show the vertical wind velocity.*

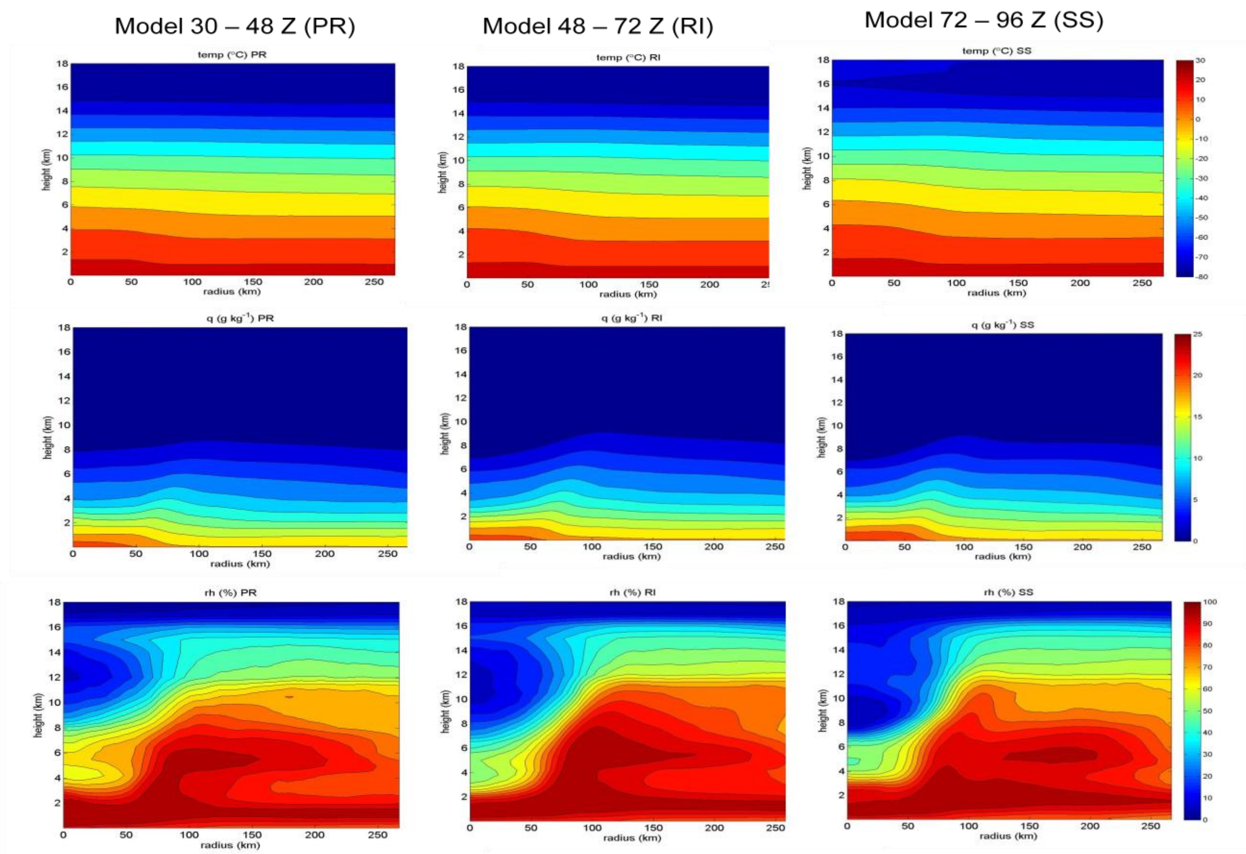


*Fig. 7: Comparison of the time-averaged simulated fields during the three stages of Bill's life cycle: PR, RI, and SS. The upper three panels show the temperature, the middle panels show the specific humidity, and the lower panels show the relative humidity.*

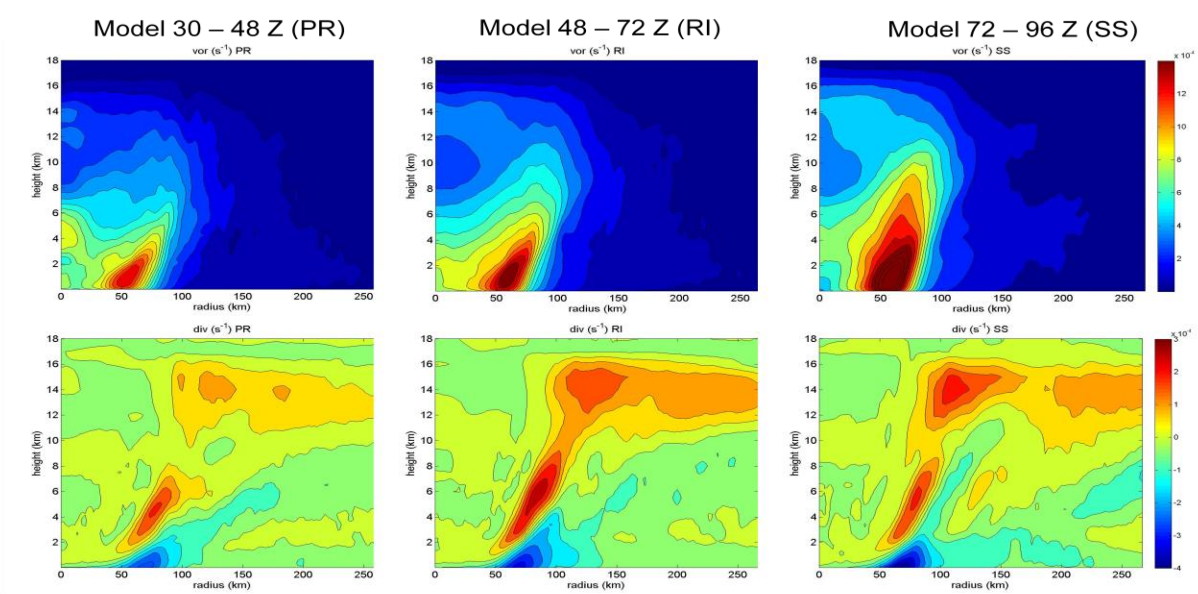


*Fig. 8: Comparison of the time-averaged fields during the three stages of Bill's life cycle: PR, RI, and SS. The upper three panels show the vorticity and the lower panels show the divergence.*

Comparisons of the time-averaged r-z mean relative vorticity and divergence during the three stages are shown in Fig. 8. It appears that vorticity becomes stronger from PR to RI and reaches a maximum during SS. The divergence immediately above the inflow layer during RI is much stronger than PR and SS.

Overall, the axisymmetric vortex-scale structures during PR, RI and SS are relatively similar.

**Surface layer fields:**

The time evolution (Hovmoller diagram) of the azimuthally-averaged surface wind speed and the sea level pressure are shown in Fig. 9. The Hovmoller diagrams of the surface layer thermal fields are shown in Fig. 10. The radial distribution of the air-sea contrasts of temperature and humidity is in general agreement with those given in the buoy composites of Cione et al. (2000).

It appears that a strong signal enhanced surface fluxes shows up right before RI. It can be seen from the axisymmetric 10-m temperature and humidity fields that dry and cool air is gradually transported from the ambient environment to the core. The large air-sea contrasts of temperature and humidity boost strong sensible and latent heat fluxes before RI. It is hypothesized that the pre-RI accumulated fluxes are one of the main mechanisms triggering the RI. Our results are consistent with that found in the Paloma (2008) case (Kaplan et al. 2010).

**Future work:**

We plan to extend the analysis of the model surface-layer fields and include an analysis of the convective-scale structure and evolution before, during, and after RI. Additional cases will also be examined, including those that have aircraft flights at all three of these stages.

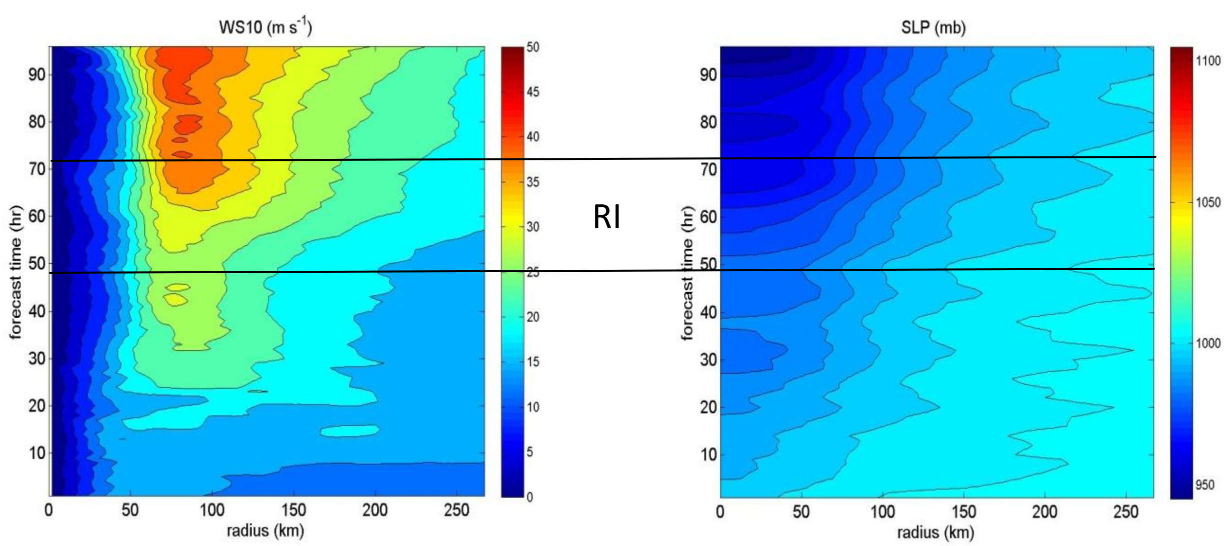


*Fig. 9: the Hovmoller diagram of the azimuthally averaged surface wind and sea level pressure. The period between the black lines is during RI.*

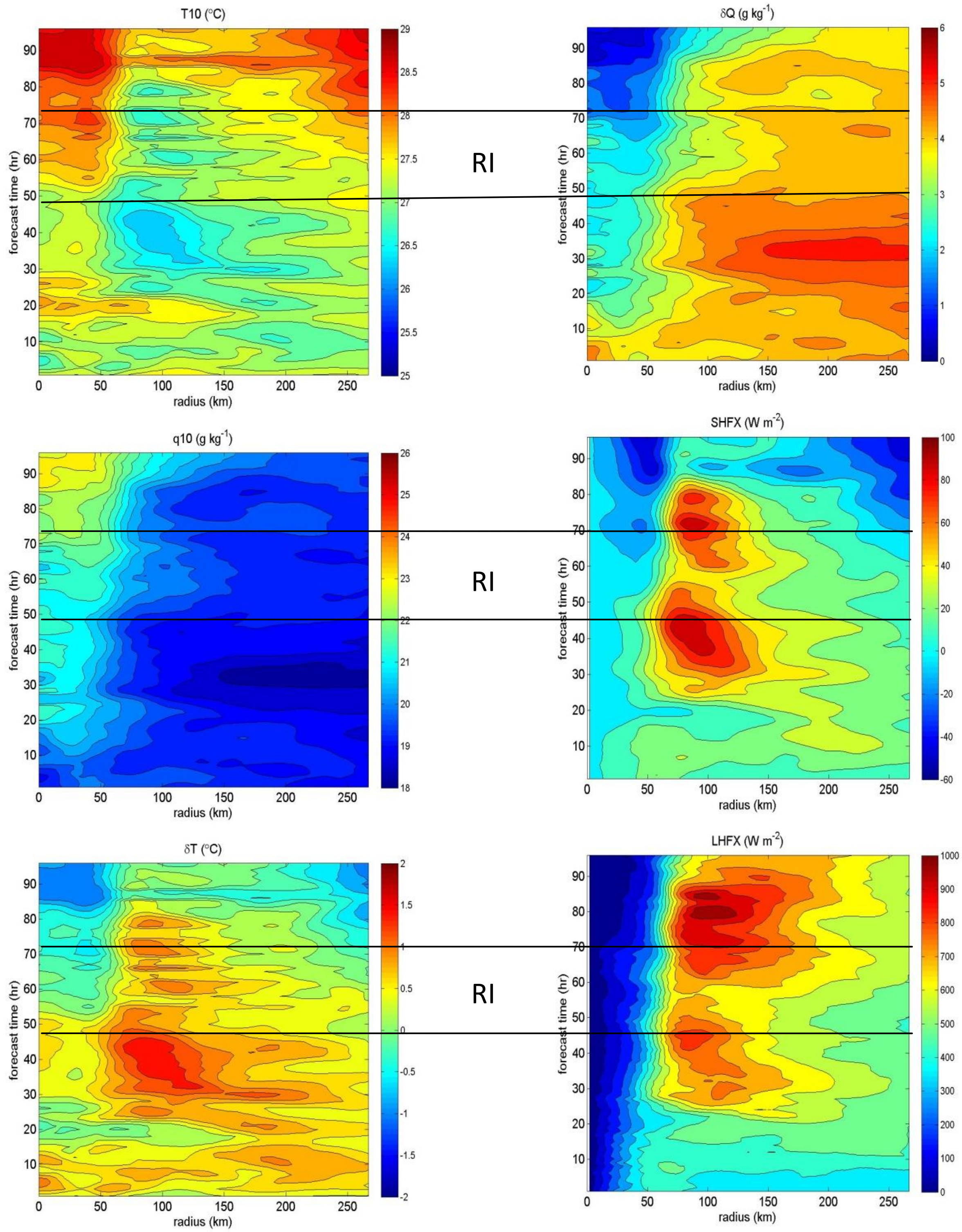


*Fig. 10: the Hovmoller diagram of the azimuthally averaged surface layer fields: 10-m temperature (T10) and specific humidity (q10), the air-sea contrast of temperature (dT) and humidity (dq), and surface sensible (SHFX) and latent (LHFX) heat fluxes. The period between the black lines is during RI.*

**References:**


Black et al. 2007: Air-sea exchange in hurricanes: Synthesis of observations from the Couple Boundary Layer Air-Sea Transfer experiment. BAMS, 88, 357-374.

Cione et al. 2000: Surface observations in the hurricane environment. Monthly Weather Review, 128,1550-1561.

Kaplan et al., 2009**:** A revised tropical cyclone rapid intensification index
for the Atlantic and East Pacific basins. Weather and Forecasting, 25, 220-241.

Kaplan et al., 2010: A multi-scale analysis of the rapid intensification of Hurricane Paloma (2008). Poster, AMS 29TH Hurricane Conference.

Kelley et al., 2004: Tall precipitation cells in tropical cyclone eyewalls are associated with tropical cyclone intensification. Geophysical Research Letters, 31(L24112).

Kossin, J.P., and M.D. Eastin, 2001: Two distinct regimes in the kinematic and thermodynamic structure of the hurricane eye and eyewall. J. Atmos. Sci., 58, 1079–1090.

Nolan et al., 2007: Tropical Cyclone Intensification from Asymmetric Convection: energetics and efficiency. J. Atmos. Sci., 64, 3377–3405.

Reasor et al., 2009: Rapidly intensifying Hurricane Guillermo (1997). Part I: low-wavenumber structure and evolution. Mon. Wea. Rev., 137, 603–631.

Rogers, R.F., 2010: Convective-scale structure and evolution during a high-resolution simulation of tropical cyclone rapid intensification. Journal of the Atmospheric Sciences, 67, 44–70.

Yeh et al., 2010: The AOML/ESRL Hurricane Research System: Performance in the 2008 Hurricane Season. J. Marine Geod., In review.

Zhang et al., 2008: First direct measurements of enthalpy flux in the hurricane boundary layer. Geophysical Research Letter, 35, L14813,dio:10.1029/2008GL034374.